Received: 9 October 2025 | Revised: 15 April 2026 | Accepted: 17 April 2026

DOI: 10.1002/esp.70298

CASE STUDY

ESPL WILEY

Geomorphological mapping of the Becca d'Aver deep-seated gravitational slope deformation (Aosta Valley, Italy) based on multi-scale and multi-sensor analysis

Alberto Bosino[1] | Francesco Barbadori[2] | Pierluigi Confuorto[2] | Danilo Godone[3,4] | Mattia De Amicis[1] | Federico Raspini[2] | Sarah Aliu[1] | Olga Nardini[2] | Ahmed Hafiz[1] | Samuel Pelacani[2] | Daniele Ferrari Trecate[3] | Michael Maerker[5,6] | Martina Cignetti[3]

[1]Department of Earth and Environmental Sciences, University of Milano-Bicocca, Milan, Italy

[2]Department of Earth Sciences, University of Florence, Florence, Italy

[3]National Research Council of Italy, Research Institute for Geo-Hydrological Protection (CNR IRPI), Torino, Italy

[4]Research Center on Natural Risk in Mountain and Hilly Environments, University of Turin, Grugliasco, Italy

[5]Department of Earth and Environmental Sciences, University of Pavia, Pavia, Italy

[6]Working Group on Soil Erosion and Feedbacks, Landscape Functioning, Leibniz Centre for Agricultural Landscape Research (ZALF), Müncheberg, Germany

Correspondence
Alberto Bosino, Department of Earth and Environmental Sciences, University of Milano-Bicocca, Piazza della Scienza 1, 20126, Milano, Italy.
Email: alberto.bosino@unimib.it

Funding information
Italian Ministry of University and Research, Grant/Award Number: 2022C2XPK7

Abstract

The aim of this work is a multi-scale, multi-sensor geomorphological characterization of the Becca d'Aver deep-seated gravitational slope deformation (DsGSD). Particular attention was given to the pseudo-badlands morphologies that crop out in the area, which are producing sediments that are subsequently reactivated by debris flows. A geomorphological map at a scale of 1:10000 was generated in the Cretaz–Comba Basset basin area, left side of the Aosta Valley in northern Italy, ending at the Champagne fan. The study area is characterized by gravitational and runoff associated processes that interact with anthropic structures. However, pseudo-badlands landforms represent the main source of sediments providing loose materials highly connected with the main drainage system. The landforms in the area were characterized and mapped using Google Earth and remote sensing interpretation as well as with field campaigns. Especially radar (Interferometric Synthetic Aperture Radar, InSAR) and optical (multispectral) data were employed to map active deformation areas and detect bare soil using the Bare Soil Index (BSI). Furthermore, we conducted a detailed terrain analysis (TA) and derived the Geological Strength Index (GSI). Moreover, we applied the connectivity index (IC) model and used remotely sensed data to assess the contribution of pseudo-badlands to the general sediment transport. The results highlight how altered bedrock materials and anthropic deposits of mined serpentinite (waste deposits) contribute to the provision of sediments that are related to hydrogeological hazard in the area.

KEYWORDS
connectivity index, DsGSD, geomorphological hazard, MorphDB, pseudo-badlands

1 | INTRODUCTION

Deep-seated gravitational slope deformations are large to giant mass movements that generally affect the entire length of valley flanks and extend to hundreds of meters in depth (Crosta, Frattini, & Agliardi, 2013, and reference therein). This type of slope deformation has been recognized worldwide as a significant process of mass wasting including a set of different morphological processes such as double-crested ridges, open or infilled trenches, downthrown blocks, ridge top depressions, graben and double or multiple ridges suggesting an extensional or mixed deformation style along the upper slope sectors (Agliardi et al., 2009; Crosta, Frattini, & Agliardi, 2013). In the Western Alps deep-seated gravitational slope deformation (DsGSD) have been known for a long time and are often associated with rocks

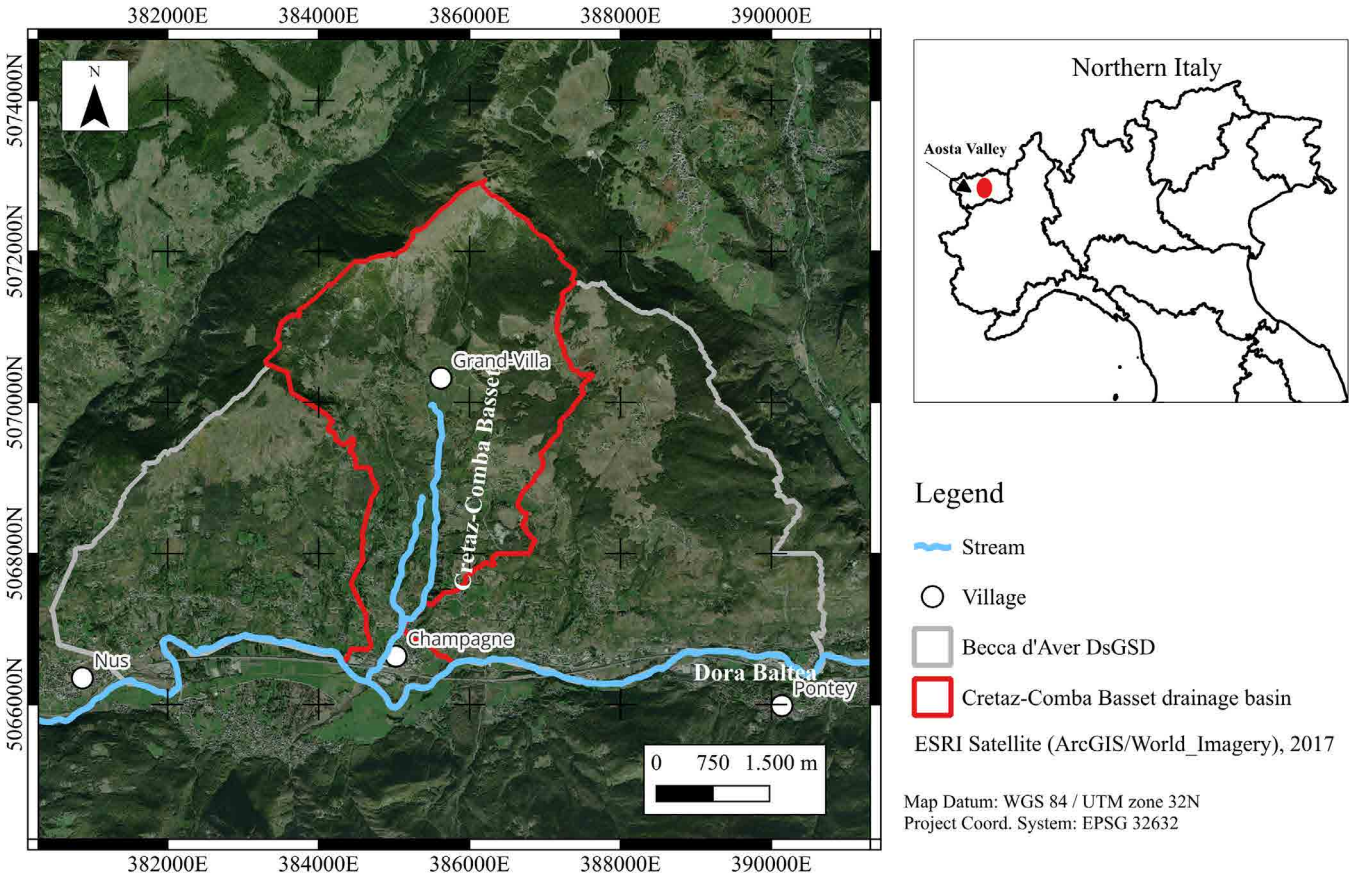

FIGURE 1 Study area.

characterized by high schistosity within highly fractured bedrock material (Cignetti et al., 2020; Crosta, Frattini, & Agliardi, 2013; Mortara & Sorzana, 1987). In general, DsGSD are slow moving phenomena having a long-term impact on anthropic structures and infrastructures (e.g., Agliardi et al., 2009; Cignetti et al., 2023b) and a morphological and morphogenetic characterization is of fundamental importance (Discenza et al., 2023). In the present paper, the Becca d'Aver DsGSD was selected for a case study (Figure 1).

The Becca d'Aver DsGSD has been studied, among others, through traditional field surveys (Carraro & Perotto, 1991) in the past. These studies indicate the origin of the deformation related to karst corrosion phenomena involving buried bodies of chalk and/or carbonate rocks, or mass slides of calcschists and ophiolites sloping towards the Aosta Valley (Dal Piaz et al., 2010). In addition, the DsGSD has been analysed with satellite images such as Landsat 5TM (Bistacchi & Massironi, 2001) and Sentinel-1 data (Cignetti et al., 2023a).

The Becca d'Aver DsGSD area has a long history of hydrogeological instability. Chronicles from the 10th and 11th centuries already report disruptions that 'formed a huge body of water in the middle of the Becca d'Aver' causing landslides and debris flows able to bury and destroy the Champagne Village (Dal Piaz et al., 2010) (Figure 1). The same area was subjected to several floods and debris events in past centuries (see historical description in Dal Piaz et al., 2010). However, nowadays the territory is still sensitive to the same processes (e.g., in April 1981 a debris flows interrupted highway 26). Many debris/mud flows and rotational/translational slides occurred during the year 2000's rainfall event (Ratto, Bonetto, & Comoglio, 2003; Giardino et al., 2013) which affected the entire region causing extensive damage and casualties.

Thus, the aim of this paper is to evaluate with a multi-scale, multi-sensor geomorphological approach the area of the Becca d'Aver DsGSD with particular emphasis on the Cretaz–Comba Basset basin, which is the drainage basin upstream of the Champagne Village (Figure 1). The study was conducted using remotely sensed data (i.e., Interferometric Synthetic Aperture Radar [InSAR]) to assess ground deformation. Moreover, multispectral analysis based on Sentinel-2 sensors was used to extract the Bare Soil Index (BSI) (Diek et al., 2017), to evaluate the bare materials that can be easily eroded by running water. Furthermore, a detailed field survey was conducted to produce a 1:10000 scale geomorphological map based on the Italian guidelines for geomorphological mapping (Campobasso et al., 2021) with the associated geomorphological database (MorphDB developed by Bosino et al., 2024) to fully characterize the landforms and deposits that are particularly prone to be reactivated and hence, flow into the stream. In general, traditional maps are static tools, suffering from temporal and scale resolution, and are commonly time-consuming, struggling to represent the complexity of the landscape on various scales and its evolution over time (e.g., Bufalini et al., 2021; Guzzetti et al., 2012; Maerker et al., 2019). In recent years digital geomorphological mapping has been consolidated (Bishop et al., 2012; Quesada-Román & Peralta-Reyes, 2023; Rączkowska & Zwoliński, 2015), the combined use of field and remote geomorphological mapping is growing, mainly integrating traditional field survey with remote sensing techniques, that is, LiDAR-based

(Jaboyedoff et al., 2012; McCerery et al., 2025), satellite-based (Siart et al., 2009; Casagli et al., 2017) and geospatial technologies (Bishop et al., 2012; La Licata et al., 2023; Reddy, 2018). Multi-scale cartography models, obtained by combining multi-sensor and multi-scale approaches, represent a modern approach to a full representation of landforms (Bufalini et al., 2021; Cignetti et al., 2025; La Licata et al., 2025). In addition, the introduction of geomorphological databases opens the possibility of easily updating the geomorphological information in each portion of the slope fully representing forms and features in time and space (Bosino et al., 2024; Forno et al., 2022).

The field survey conducted in the area revealed that the weakness of the bedrock in the Becca d'Aver study area is responsible for the development of badland-like landforms, which are characterized by accelerated erosion and are closely linked to the Cretaz–Comba Basset stream. Badlands had been defined as 'intensely dissected natural landscapes where vegetation is sparse or absent and which are useless for agriculture, typically considered of fluvial origin, characterized by very high drainage densities, V-shaped valley and short, steep slopes' (Bryan & Yair, 1982). Usually, badlands represent one of the most complex soil erosion landforms and are described as classic polygenic landform (Battaglia, Leoni, & Sartori, 2002; La Licata et al., 2023). Even if badlands are usually formed in soft sedimentary rocks (i.e., marls and mélange) or in colluvial materials (e.g., Aljinović et al., 2010; Bufalini, Omran, & Bosino, 2022; Moreno-de las Heras & Gallart, 2018), highly fractured and altered rocks as well as glacial deposits may show badlands-like features and associated runoff process (Bollati et al., 2017). In the study area, we decided to name these landforms as 'pseudo-badlands' because they are shaped by a combination of runoff and slope-associated erosive processes affecting metamorphic rocks that lead to badlands morphology. In fact, deep rill-interrill erosion and retrogressive erosion up to the watershed divide produce classic knife-shaped slopes (Moretti & Rodolfi, 2000). In addition, these landforms are morphologically characterized by steep slopes and are affected by rills, gullies, rockfall and mantled by talus feed and scree slopes in weak fractured metamorphic (serpentinite) rocks. Also, Rizzo et al. (2023) and Ferrando, Faccini, & Coratza (2024) cited pseudo-badlands morphology associated to serpentinites cropping out in ophiolitic units respectively in the southern and northern Apennines. The pseudo-badlands in our study area are not the same morphotype of Badlands Type C or the so-called pseudo-badlands described by Coratza & Parenti (2021), which refers to Apennine badlands cropping out in soft sedimentary rocks. Moreover, they are not congruent with the ones defined by Bollati et al. (2019), Bollati et al. (2024) and Coratza et al., 2021 that represents complex gully systems respectively in glacial and moraine deposits. Cornamusini et al. (2009) and Bianchini et al. (2025) associate other types of pseudo-badlands with earth/mudflows. Finally, badlands-like landforms can consist of different types of rocks not classically associated with badlands: false-badlands and pseudo-badlands were described by Dill et al. (2020). However, these landforms are morphologically different from the pseudo-badland landforms cropping out in the Becca d'Aver study site due to the lithological characteristics of the bedrocks.

Pseudo-badlands are responsible for most of the sediment production in the area. However, it should be considered that the DsGSD slope is further characterized by more than twenty active and inactive serpentinite quarries. In the past, the quarried serpentinite (waste deposits) was stored and abandoned close to the excavation sites and nowadays these materials represent sediments available to be transported by surface waters and debris flow events. To fully understand the contribution of landforms and deposits in the sediment production, we conducted a detailed geomorphological survey and derived the Geological Strength Index (GSI) (Marinos, Marinos, & Hoek, 2007) as well as the connectivity index (IC) (Cavalli et al., 2013) to evaluate the degree of bedrock fracturing as well as the sediment connectivity.

This study contributes to the understanding of the general geomorphological dynamics of an area that is highly affected by different processes acting at various spatial and temporal scales. We also detected and defined geomorphic hazards in the area.

2 | METHODS

The methodology followed in this study is represented in (Figure 2) and consists of a series of steps to characterize the area from slope to site scale.

2.1 | Study area characterization with remote sensing data and terrain analysis

2.1.1 | Study area description

The Becca d'Aver study area corresponds to a slow-moving, deep-seated phenomenon, extending over 30 km^2, in the central portion of the Aosta Valley, a small alpine region of the Western Italian Alps (Figure 1).

The DsGSD corresponds to a giant triangular-shaped slope extended from the Becca d'Aver peak (2468 m a.s.l.) to the main valley bottom, between the municipalities of Nus and Pontey, along the Dora Baltea River. The outcropping bedrock is part of the Piedmont Nappe System, a tectonic-metamorphic unit composed of a complex pile of nappes, which presents post-collisional tectonic activity followed by a neo-tectonic dislocation system activation (Aosta-Ranzola fault system, Bistacchi et al., 2001), a result of extensional tectonics associated with hydrothermal activity. The DsGSD feature is controlled by faults and joints oriented in NE–SW and NW–SE directions (Bistacchi & Massironi, 2001). The principal lithologies outcropping are undifferentiated calcschists, prasinites, serpentinites and ophicalces, serpentinitic breccias in carbonate matrix, pertaining to the Combin Unit (Servizio Geologico d'Italia, 2010). At the base of this unit a thin tectono-stratigraphic unit of terrestrial origin is present, that is, the Pancherot-Cime Bianche Unit, separated from the Zermatt-Saas Unit by a thrust system on the eastern edge of the Becca d'Aver slope.

The whole slope shows a glacial footprint, related to the Balteo Glacier dynamics (middle-upper Pleistocene) that moulded the valley flanks into a series of slope breaks (Gianotti et al., 2008). This shape is emphasized by the Becca d'Aver deep-seated phenomenon that affects the entire valley flank, differentiating the slope into a series of terraces, unordered and not laterally continuous, indicating an overlay of DsGSD deformation on glacial-derived forms. Watercourses are superimposed on the glacial landforms, showing a distinct DsGSD control over the general drainage pattern. Most of the area is drained

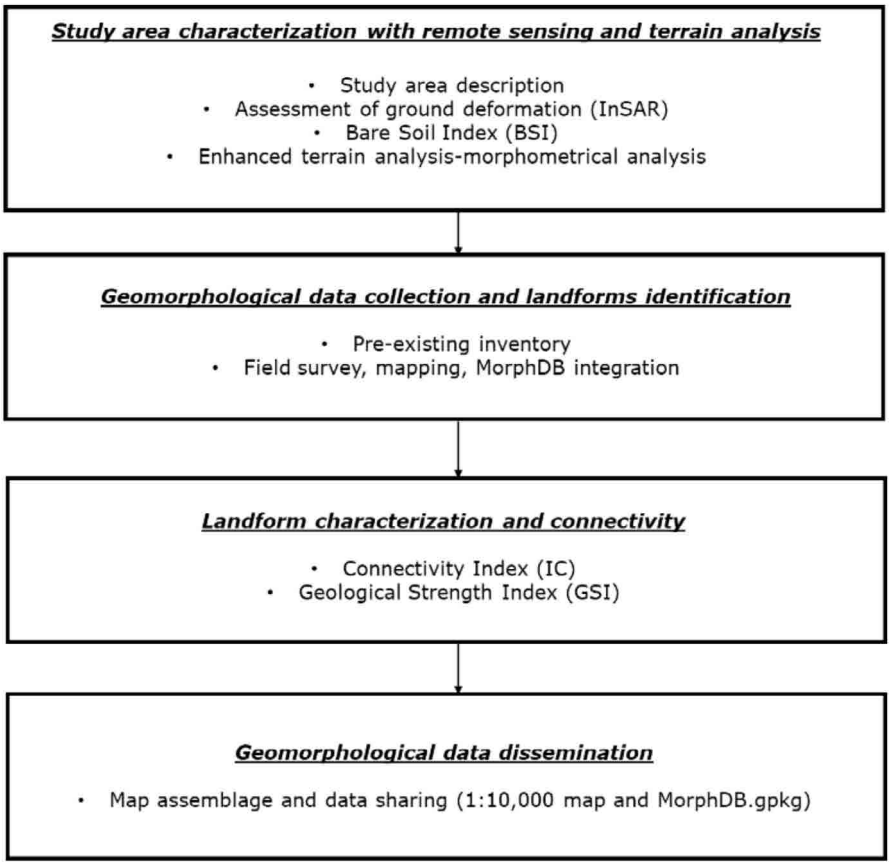

FIGURE 2 Methodological flowchart.

by a complex river network, which flows from N to S, characterized by deeply embedded sectors alternating with sectors with gently slopes without any erosional activity. This is particularly evident in the middle-lower portion of the slope, within the Cretaz–Comba Basset basin (11.5 km^2), mainly downstream Moulin locality, between Moulin and Dorinaz localities, and upstream of Grand-Villa hamlet. These morphological steps are highly incised to form deep gorges and pseudo-badlands, with steep slopes (45°–50°). Along these sectors, bedrock is highly fractured and often poorly interlinked to heavily broken rock masses or totally collapsed outcrops, mainly consisting of serpentinite breccias in carbonate matrix, belonging to the Combin Unit. Along the steepest sectors, the highly fractured rock masses, showing increased erodibility, constitute an important source for solid transport along the drainage network, activated by local rotational slides or, during intense rainfall events, important debris flows and landslides phenomena. These types of landslides affect the Becca d'Aver slope in various ways and represent a prevalent distribution in the area close to the Grand-Villa hamlet, and along with the strongly incised hydrographic network of the middle-lower portions of the slope, providing debris material to the alluvial fans of the valley bottom.

2.1.2 | Assessment of ground deformation (InSAR)

The SAR satellites constellation Sentinel-1 (EU Copernicus programme) was initially employed in this study to investigate ground deformations of the DsGSD using the InSAR technique (Hilley et al., 2004; Fialko et al., 2005; Bell et al., 2007; Chaussard et al., 2014; Fiaschi & Wdowinski, 2020). The radar sensors' acquisition geometry registers two distinct velocities along the Line of Sight (LOS) in ascending and descending geometry, measuring the relative ground-satellite distance and building up a time series (TS) database. The descending and ascending datasets may be decomposed and combined to obtain the east–west and vertical components of the movement. In this work, InSAR data (both LOS velocity datasets and EW and vertical components) were collected from the European Ground Motion Service (EGMS, Crosetto et al., 2020, https://land.copernicus.eu/en) using the EGMStream App (Festa & Del Soldato, 2023) covering the period between 2019 and 2023. LOS velocity datasets were used to identify and characterize the entity of displacement of the various sectors, particularly detecting high-velocity areas and stable portions of the slope.

EW and vertical components TS, also available from EGMS, were used to carry out an advanced analysis of the segmentation of the DsGSD body using principal component analysis (PCA) and the K-means clustering algorithm, which improves the identification and categorization of various deformation patterns (Festa & Del Soldato, 2023). When applied to TS-InSAR datasets, Principal Components (PCs) are extracted to maximize variance and characterize spatial–temporal deformation patterns without prior constraints (Chaussard & Farr, 2019). After normalization of the TS-InSAR dataset, PCA was applied to identify components with the highest variance and the K-Means unsupervised clustering algorithm was employed to group principal components TSs with similar characteristics together (e.g., linear displacement with positive acceleration, linear displacement with positive velocity and stable linear trend).

2.1.3 | BSI

The Sentinel-2 data (EU Copernicus programme) were used in this study. The multispectral sensor allows detection of surface materials through reflected light across 12 spectral bands between 400 and 2500 nm. In particular, the bands' reflectance values can be combined to calculate spectral indices that indirectly estimate the relative quantity of a surface property or material. In this study, the BSI (Diek et al., 2017) was considered because it is one of the most useful spectral indices to detect bare soil areas (susceptible to erosional processes) and to estimate the bareness intensity (from mixed bare soil with sparse vegetation to extensively bare soil). Bare soils in the study area are mainly related to pseudo-badland forms and features or gravitational deposits that can be activated or remobilized during extreme meteorological events. The BSI was calculated using the following formula using the blue (490 nm), the red (665 nm), the near infrared (842 nm) and the SWIR (1610 nm) bands:

$$\mathrm{BSI} = \frac{((\mathrm{red} + \mathrm{SWIR}) - (\mathrm{NIR} + \mathrm{blue}))}{((\mathrm{red} + \mathrm{SWIR}) + (\mathrm{NIR} + \mathrm{blue}))}$$

The BSI was calculated from the image acquired on 21 February 2023 and was then reclassified into four qualitative classes using the 25th, 50th and 75th percentile of the distribution to obtain a clearer view of areas with increasing spectral intensity of bare soil.

2.1.4 | Enhanced terrain analysis-morphometrical analysis

A morphometric characterization of the entire slope was performed using a high-resolution digital terrain model (DTM) that represents the surface shape without tree and anthropic elements, representing the proper cartographic layer to carry out a morphological and morphometric analysis (Guth et al., 2021). This LiDAR-derived DTM (2 × 2-m cell) was acquired in 2008 and is made available by regional authorities on the SCT Geoportal (https://geoportale.regione.vda.it/download/dtm/). Operating in a GIS environment, a preliminary terrain analysis (TA) was carried out by deriving the primary terrain attributes from the DTM (e.g., slope, aspect and elevation) and some representative terrain indices (e.g., slope position, terrain dissection and stream power index [SPI]), to morphometrically characterize the entire slope and to remotely map and extract the diverse landforms (Table 1).

TABLE 1 DTM derivatives.

Topographic index	References
Slope	Zevenbergen and Thorne (1987)
Aspect	Zevenbergen and Thorne (1987)
Elevation	Wang and Liu (2006)
Slope position	Boehner and Selige (2006)
Terrain dissection	ESRI (2011)
SPI	Moore, Grayson and Ladson (1991)

2.2 | Geomorphological data collection and landforms identification

To fully characterize the area from a geomorphological point of view, pre-existing data were assessed and downloaded from open-source databases. The database associated with the geological data of the 1:50000 scale geological map (Sheet 091-Chatillon; Servizio Geologico d'Italia, 2010) were downloaded from the CARG GATE (https://progetto-carg.isprambiente.it/cartografiaCARG/cartageologica.php?regione=Valle+d%27Aosta&foglio=091) (accessed on April 2024). In addition, from the Aosta Valley Geoportal (https://geoportale.regione.vda.it/) the 1.10000 topographic map (CTR-year 2003) and the layer called 'Catasto dissesti', including the Inventory of Landslide Phenomena in Italy (IFFI) data at a scale of 1:10000 was considered. Moreover, we downloaded information from the ISPRA IdroGEO geoportal (https://idrogeo.isprambiente.it/app/page/open-data) and respectively assessed it.

Furthermore, dedicated field surveys were conducted in July and October 2024 to check and update the landforms geometry as well as to survey landforms associated with the DsGSD following the legend proposed by Campobasso et al. (2021). Particular attention was given to pseudo-badlands forms and features as well as waste deposits due to the high relation with the geomorphological hazard in the area. The field surveys were conducted at a 1:10000 scale, and a GIS-based mapping procedure was conducted using a DELL Latitude 7220 Rugged Extreme Tablet. Finally, recent Google Earth images and stereophotos acquired from the IGM (https://www.igmi.org/) of the year 1996 and 2004 were analysed, refining the geomorphological survey.

The geomorphological data from the surveys were elaborated using QGIS (Version 3.40) and integrated in the MorphDB structure (Bosino et al., 2024).

2.3 | Landform characterization and analysis

2.3.1 | IC

To characterize the sediment connectivity of the pseudo-badlands of the Cretaz–Comba Basset basin, the IC improved by Cavalli et al. (2013) was computed. Leveraging Sedin Connect (Crema & Cavalli, 2018) stand-alone open-source tool, the IC was derived from the 2-m-DTM to (i) characterize the morphology of river systems, (ii) assess the sediment transport and deposition and (iii) analyse new potential connectivity pattern with respect to debris flow occurrence. In accordance with Cavalli et al., 2013, we imposed as parameter setting the local measure of topographic surface roughness, that is, a roughness index (RI), as the weighting factor W. The use of a RI in the IC result is more suitable for alpine catchments application and better represent the large unvegetated areas with different surface roughness depending on the characteristics of outcropping rock and debris cover. It is more suited for modelling sediment transfer by debris flows, which is an active phenomenon in sediment-related processes in Alpine basins. Having a high-resolution regional LiDAR available, the unmodified DTM was used without filling local depressions (Crema & Cavalli, 2018), thus using the original morphology to analyse the existent textural roughness. Anthropic infrastructure as water regulation works (e.g., check dams) very widespread in the basin, were

kept in the model to account for their influence in impeding or modifying the flow regime.

2.3.2 | GSI

At site scale, the GSI (Marinos, Marinos, & Hoek, 2007) was derived to evaluate the fracture conditions of bedrock characterized by pseudo-badlands morphologies. The GSI is based on the assessment of lithology, structure and discontinuity conditions of the bedrock and provides a visual examination of rock mass in the field. The blockiness and discontinuity of the mass are directly related to the potential for erosion by both gravity and flowing water, contributing to the production of debris that could be connected to the main drainage and transported downstream. Even if GSI has some limitations to represent vulnerability to erosion in an applicative context (Pells et al., 2017), the index helps us to define the potential for erodibility specifically for those areas characterized by highly fractured and poorly interlocked outcrops.

2.4 | Geomorphological data dissemination

The geomorphological map was compiled at a scale of 1:10000 (supporting information) following Campobasso et al., 2021 and covering in the MorphDB structure (Bosino et al., 2024). The MorphDB allows the representation of all the geomorphological elements present on the slope, allowing a full and accurate geomorphological representation of the data. The database associated with the landforms, reflected in the legend of the map, is divided into L&D_polygon, L&D_polyline and L&D_points. The BL_polygon units were added to represent the geological outcrops surveyed by Servizio Geologico d'Italia (2010).

The final map shows the level LFD that represents the highest mappable landforms (Bosino et al., 2024). In addition, three boxes reporting LFD-1 and LFD-2 were reported and compared to the LFD level. Finally, a set of representative landforms is reported on the map. The symbols used to represent the landforms fit best those proposed by Campobasso et al., 2021. However, the database allowing for a detailed representation of the landforms and processes at different hierarchical levels was shared in the supporting information (MorphDB.gpkg).

3 | RESULTS

3.1 | DsGSD-scale InSAR analysis

The deformation maps (Figure 3) show generally very low values of deformation, with most of the PS displayed in green or yellow/light blue, indicating that most of the PS are within or close to the stability interval. It should be remarked that the north–south exposition of the Becca d'Aver area is not particularly favourable for the detection of movement with current satellite platforms, that are almost blind to this component of movement. However, even though the technique has its limitations, InSAR is the only monitoring tool in the area for this type of slow deformation phenomenon.

The mean velocity for all the points considered in the ascending geometry is −0.14 mm/year, with a minimum of −2.95 mm/year and a maximum of 1 mm/year. For the descending geometry, the mean is 0.09 mm/year, with the minimum at −2.95 mm/year and a maximum at 1.3 mm/year. These values confirm the very slow movement of the sectors. Notably, a small sector in the central part of the area, circled in red, shows detectable movement with a maximum of 3.9 mm/year and a minimum of −6.6 mm/year in the descending geometry and a maximum of 6.2 mm/year and a minimum of −11 mm/year in the ascending one. Another sector in the upper part of the area, in the white circle, visible in both geometries, presents higher values. In the descending geometry, this sector records a maximum of 0.6 mm/year and a minimum of −9.1 mm/year, while in the ascending geometry, a maximum of 2.4 mm/year and a minimum of −8.1 mm/year.

Figure 4 shows the result of the PCA for the EW (left side) and Vertical (right side) components. The PCA applied to the EW components and identified four different clusters. In the upper part of the figure, different sectors of the area, which have similar behaviour and velocities, are identified by different names and colours: EW-1 in red and EW-2 in yellow in the central part of the area; EW-3 in light blue and EW-4 in blue in the southern, western and northern sectors. The

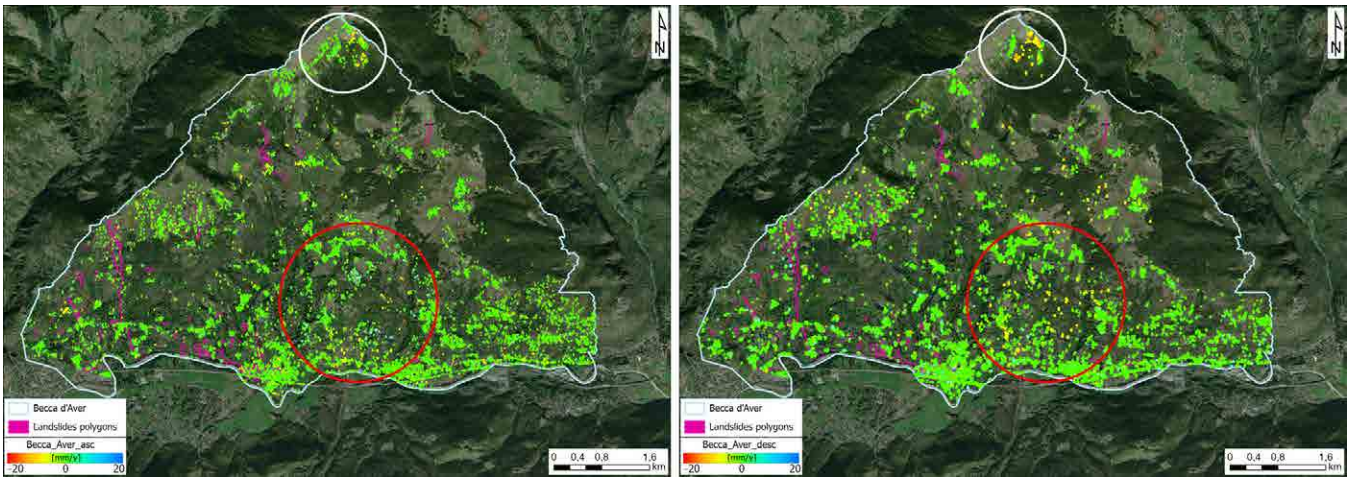

FIGURE 3 Ascending, on the left, and descending on the right, Interferometric Synthetic Aperture Radar (InSAR) results of the Becca d'Aver area (highlighted in light blue) with fast-movement landslides polygons in pink. The data come from the EGMS for the 2019–2023 period (high local velocity sectors are represented by white and red circles).

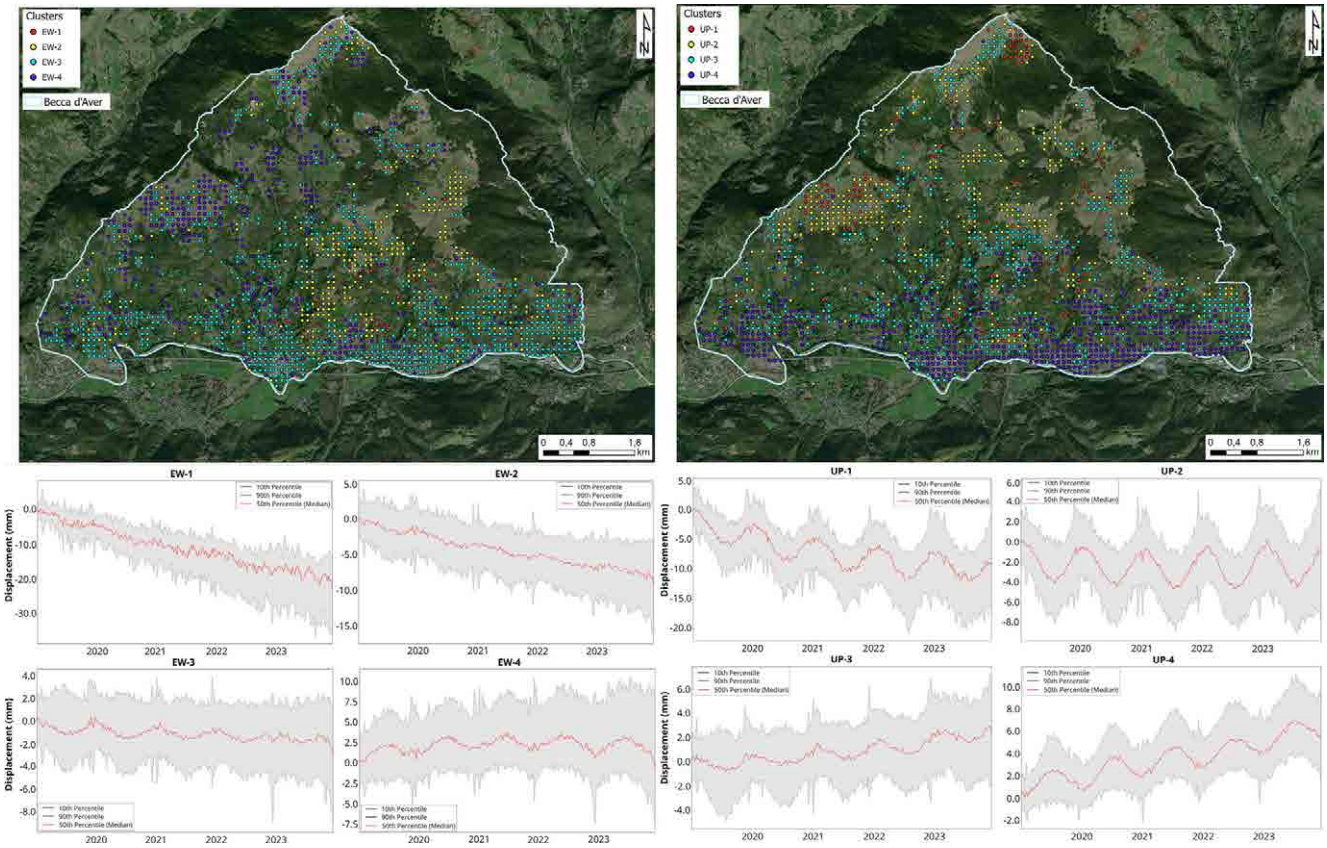

FIGURE 4 Principal component analysis (PCA) results for the Becca d'Aver area, for the EW (left side) and vertical (right side) components. Localization of the different sectors identified (EW-1; EW-2; EW-3 and EW-4, UP-1; UP-2; UP-3 and UP-4) in the upper part, and clusters in the lower part, one for each sector identified.

lower part of the image shows clusters of velocities for each identified sector. EW-1 shows a relatively linear shift of up to −20 mm over a 5-year period (from 2019 to 2024), indicating the strongest movement of the area, and EW-2 shows a much smaller shift, about −10 mm/5 years (2 mm/year), both towards the west. EW-3 and EW-4, which cover most of the area, show only minimal shifts over the same period, indicating very low seasonality. Also, for the Vertical components, four different clusters were identified. UP-1 in red, UP-2 in yellow; UP-3 in light blue and UP-4 in blue (Figure 4). The lower part shows the different corresponding velocity clusters of each sector. All four clusters show an oscillating seasonal trend. UP-1 is the cluster with the highest displacement values, about −10 mm in 5 years, and shows a downward trend, while UP-2 shows only an oscillating trend with no significant displacement. In addition, the UP-3 and UP-4 clusters show a positive (upward) oscillating trend with displacement values of around 2 and 5 mm, respectively, over the same period. As can be seen in (Figure 4), the upper sectors of the slope are characterized by vertical displacement in the downward direction (cluster UP-1). In the middle sectors, horizontal movements become relevant with a westward direction in this case (clusters EW-1 and EW-2). Finally, in the lower parts, the vertical displacement shows an upward direction (clusters UP-3 and UP-4).

3.2 | DsGSD-scale BSI derivation

Figure 5 presents the multispectral results of the Becca d'Aver area, characterized by the four-level spectral intensity classification of the BSI. The southeastern and southwestern sectors of the area are marked by high and very high BSI intensity, as evidenced by the two big red sectors, while the northern part predominantly displays lower-intensity values. The central sector exhibits more variable results, with both low and high BSI intensities. This variability of results may also be influenced by the acquisition period, during February, a period with a limited presence of vegetation. The maximum value recorded of BSI intensity in this area is 1, and the mean value is 0.196.

3.3 | DsGSD-scale TA

To morphometrical characterize the slope affected by the Becca d'Aver DsGSD and its interrelation with pseudo-badland landforms, a morphometric characterization of the entire slope was carried out, to focus on the soil erosion processes and their dynamics. Figure 6 shows the main DTM-derived products and indices from the regional 2-m DTM. The mountain side affected by the Becca d'Aver DsGSD ranges between 438 and 2586 m a.s.l., with a main south-facing slope. The upstream portion, set in outcropping bedrock, shows an extremely steep slope (35°–45°); the rest of the slope is characterized by extended gentle slope sectors (0°–15°), corresponding to ancient glacial terraces dislocated by a series of medium to steep scarps (25°–35°, 35°–45°). The medium-lower portion of the DsGSD presents a steeper slope characterized by a dense, north–south oriented, hydrographic network.

The slope position, providing the measure of slope position from the valley bottom to the ridge, is useful to determine if the elevation

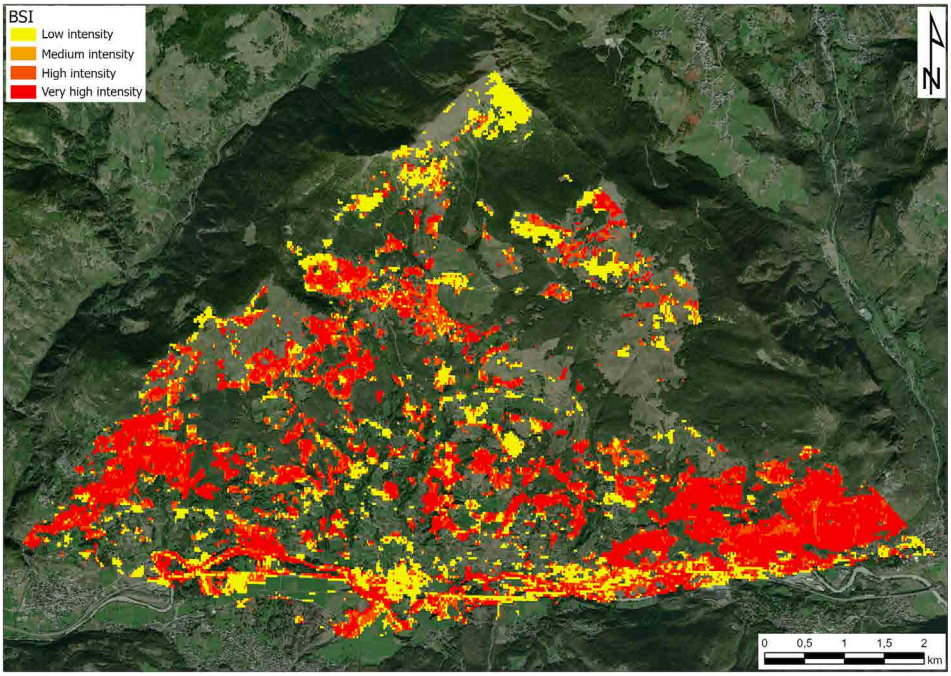

FIGURE 5 Bare soil index of the Becca d'Aver (Aosta Valley) reclassified into four main classes: low intensity, medium intensity, high intensity and very high intensity.

is higher or lower than the mean of the neighbourhood, allowing the delineation of main scarps and terraces along the entire slope, as well as the main river incisions and the deeply embedded sectors characterizing the middle-lower portion of the slope. Terrain dissection, the measure of how incised the landscape is at the cell location, proves useful for extrapolating erosional scarps along the main river incisions, mainly in correspondence of the pseudo-badland sectors, as well as to define and extract several linear morpho-structural elements such as double or multiple ridges, scarps and counterscarps, open or infilled trenches, characterizing the large deep phenomena. The SPI corresponds to the measure of the erosive power of concentrated flowing water, showing high values in the drainage area and in the pseudo-badland forms.

3.4 | Basin-scale geomorphological mapping and MorphDB implementation

The landforms were identified and grouped based on the main morphogenetic processes following Campobasso et al., 2021: (i) litho-structural, (ii) gravitational, (iii) glacial, (iv) periglacial and nival, (v) fluvial and runoff associated and (vi) anthropogenic landforms.

3.4.1 | Litho-structural landforms

The litho-structural landforms crop out only in the north part of the study. In fact, that sector is characterized by the presence of structural selective scarps that correspond to the head of the strata of ophicalcite rocks cropping out at the watershed.

3.4.2 | Gravitational landforms

The entire slope is characterized by the Becca d'Aver DsGSD. This phenomenon causes several morphological evidence-like terraced areas and scarps (main map, Figure 5 and supporting information). In addition, the area has complex and undifferentiated landslides as well as rotational landslides, debris flows and rockfalls. Undifferentiated landslides are activated starting from scree slope deposits that widely mantle the study area but also persist in the northern part of the area, affecting the relief. In the same area, several debris flow channels highlight the contribution of debris to morphogenesis. North of the village of Gran Villa, two suspended fans formed by fluvial processes and debris flows lie at the base of the relief, indicating the activity of morphogenesis in the area. Moreover, the fan of Champagne in the lower part of the study area is also largely characterized by the presence of debris flow deposits, and in the years, a sand quarry was built up.

3.4.3 | Glacial landforms

Glacial deposits mantle the slope in the middle to lower part of the area. These deposits are heterometric and lithologically heterogeneous representing lateral glacial deposits associated to the last glacial maximum (Upper Pleistocene). These deposits are prone to be eroded by surface runoff forming biancane-like landforms (main map, Figure 4 and supporting information). Glacial deposits contribute to the sediment budget of the main drainage passing the Champagne Village.

3.4.4 | Periglacial and Nival landforms

In the north part of the study area, nival avalanche tracks are highlighted by small longitudinal depressions and absence of vegetation (main map, Figure 6 and supporting information).

3.4.5 | Fluvial and runoff associated landforms

Pseudo-badlands represent the most important evidence of water runoff in the area (main map, Figure 3 and supporting information).

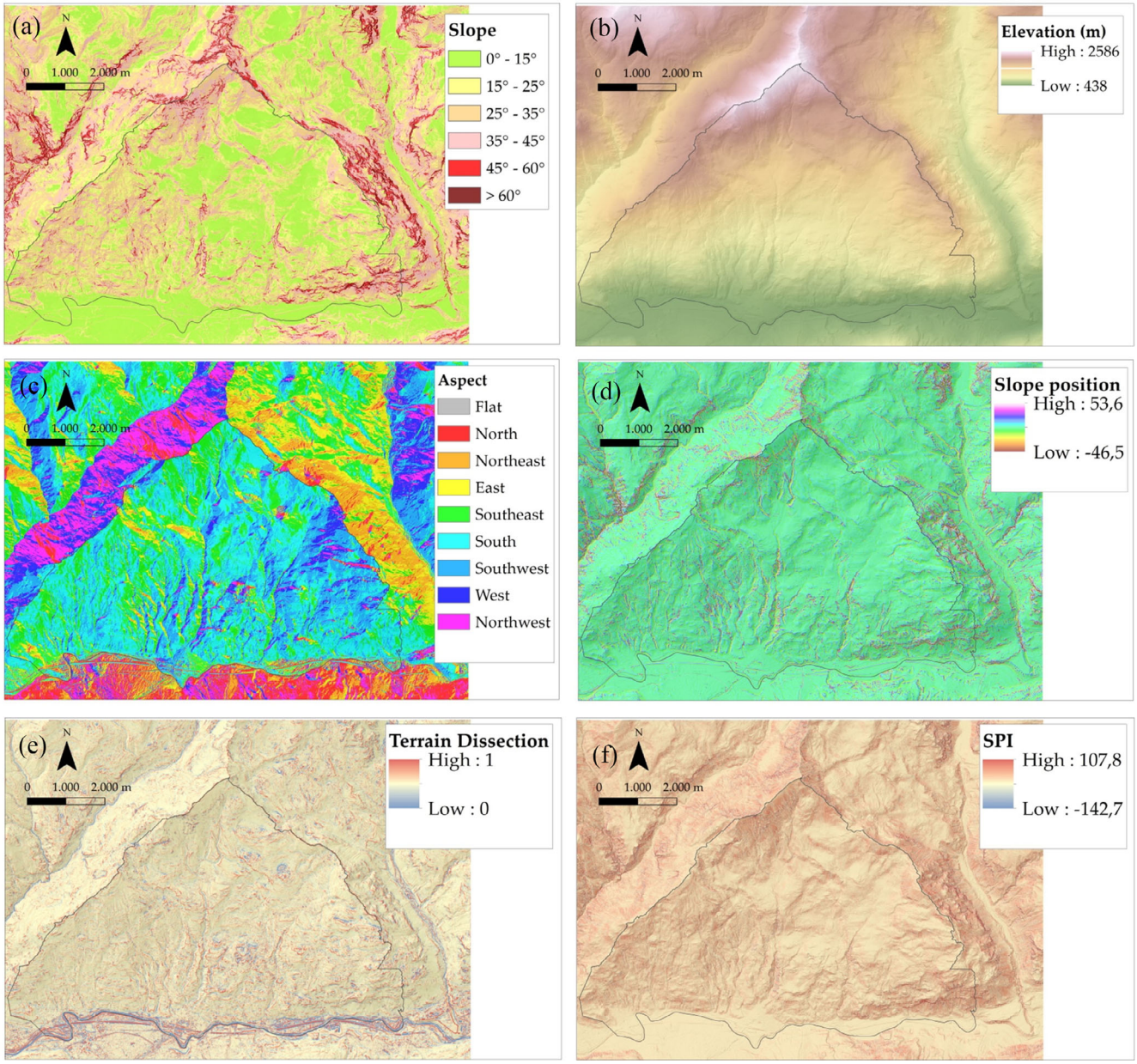

FIGURE 6 Terrain analysis of the Becca d'Aver DsGSD, (a) slope, (b) elevation, (c) aspect, (d) slope position, (e) terrain dissection and (f) stream power index.

These polygenic landforms are the result of the combination of slope and runoff processes acting on deeply fractured serpentinites covered by glacial deposits. They are delimited on top by denudation scarps and are shaped by rill-interrill erosion, rockfalls and mantled by scree slope deposits. These landforms contributed to producing the material activable as debris flow, which is an expression of the slow and protracted evolution of the DsGSD. Associated with the denudation scarps, we find fine glacial deposits eroded by surface runoff, producing biancane-like landforms (main map, Figure 4 and supporting information). Moreover, the area is widely characterized by colluvial talus deposits which mantle the topography. In addition, peat bogs are observed in flat areas along the slope. Finally, the area has many water spring niches directly correlated with the DsGSD.

3.4.6 | Anthropogenic landforms

In the area, active and inactive serpentinite quarry represents the main anthropogenic element that shapes the earth's surface (main map, Figure 1 and supporting information). In addition, several check dams (main map, Figure 2 and supporting information) are placed in the main drainage system to preserve the village of Champagne from potential debris flow that could be activated starting from anthropic deposits of mined serpentinite as well as debris flow activated in scree slope deposits. Along the main roads in the area, several retaining walls have also been placed to reduce the landslide risk.

In addition, the surveyed geomorphological data have been implemented in the MorphDB structure (Bosino et al., 2024) to fully represent all the landforms that characterized the Cretaz–Comba

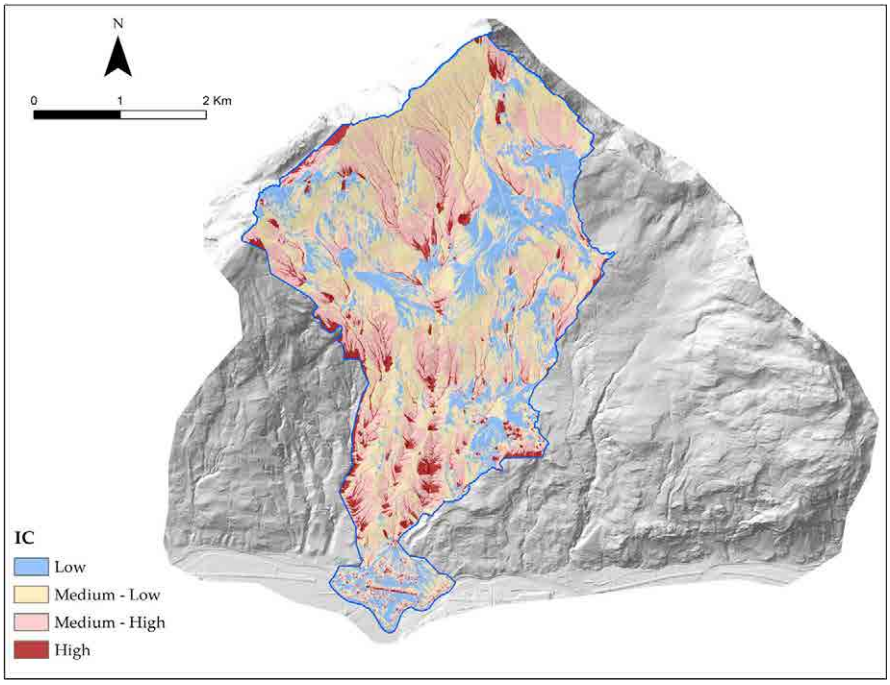

FIGURE 7 Connectivity index (IC) computed at the scale of the Comba Basset basin showing the pseudo-badlands in the middle-lower portion of the basin characterized by medium-high and high IC classes, and the low IC value corresponding to depositional sector most prone to debris flow accumulation.

Basset basin. The MorphDB overcomes these issues by allowing the representation of each portion of the slope processes acting at different spatial–temporal scales. The geomorphological elements were mainly mapped as polygons. Due to scale issues, lines and points were also reported. On the main map (supporting information—Boxes A, B and C), we present the three levels of the MorphDB. In this case the level LFD-2 (Box A) shows the slope affected by the lower landforms (i.e., DsGSD), which affect the entire slope. On the top of the landslide a series of glacial deposits are presents (LFD-1—Box B) that are further colluviated by slope processes (LFD level—Box C).

3.5 | Basin-scale IC analysis

Analysing the potential sediment fluxes magnitude to the main network can represent a key element to manage the consequences in those kinds of mountain catchments, often characterized by frequent debris flow phenomena. The estimation of sediment fluxes magnitude in fact helps to an efficient management and evaluation of risk reduction strategies and watershed management. In order to assess the areas well connected within the main drainage of the area, the IC of the Cretaz–Comba Basset catchment was computed. The IC pattern (Figure 7) shows a strong correspondence with geological and morphological settings of the basin. This pattern reflects the high complexity of the basin characterized by a surface runoff closely influenced by the level of fracturing or looseness of the rock mass. In the upstream portion of the catchment, the extensive outcropping bedrock, mainly consisting of mylonitic serpentinite outcrops characterized by a high degree of fracturing, acts as a coupling factor due to both geological setting and geomorphic action of the dense channels acting as efficient sediment transport to the gentler slope sectors at the base of the rock walls. These sectors in the middle-high portion of the basin, characterized by low-IC values, correspond to areas potentially most prone to debris flow accumulation. In the middle-lower portion of the catchment, which is dominated by pseudo-badlands, the steep-slope portion of these deeply embedded sectors exhibits high to medium-high connectivity. These sectors demonstrate evident coupling behaviour, favouring high sediment transport that converges towards the large mixed fan on the valley floor surrounding Champagne.

3.6 | Site-scale characterization with GSI

The GSI analysis was conducted in five representative points withing the pseudo-badlands landforms. The serpentinites that characterize the area are very blocky and highly weathered (e.g. main map, Figures 1, 3 and 4 and supporting information); thus the GIS is between 30 and 35 ± 5, indicating poor structural strength and high erodibility (Figure 8). The structure of the bedrock favours the slope-associated processes producing the materials, for example, talus fees and blocks in the drainage that will be activated as debris flow.

4 | DISCUSSION AND CONCLUSION

This work integrates traditional geomorphological maps with full-coverage, multi-scale and multi-temporal approaches which are based on field surveys and detailed TA, as well as remotely sensed data. This provides an effective and complete understanding of the interrelation of landscape evolution, landforms and processes. A multi-strata geomorphological database (MorphDB, Bosino et al., 2024) was implemented to hierarchically represent the observed landforms. Each landform is associated with geomorphological information and morphometric evidence easily accessible and searchable. This approach was applied for the Becca d'Aver slope investigation, leading to a large DsGSD characterized by a progressive and continuous displacement that dissects the slope, overlapping glacial-derived landforms and acting on the watercourses drainage system.

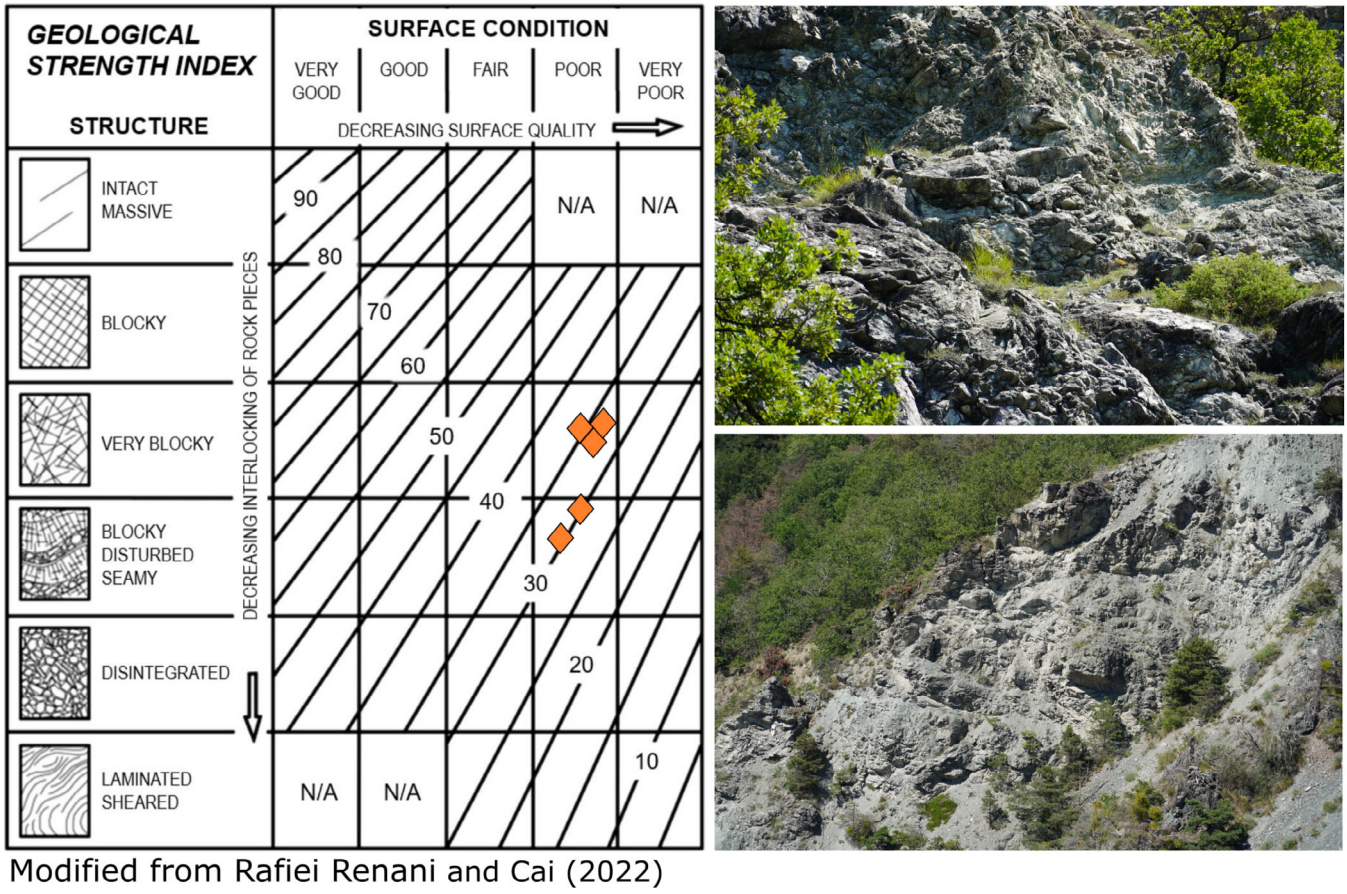

FIGURE 8 Geological Strength Index (GSI) applied on pseudo-badlands serpentines. Points locations are on the main map.

To support geomorphological characterization, remote sensing data demonstrated an important role in defining peculiar aspects. The deep movement of the Becca d'Aver can be described as a roto-translation, a distinctive deformation pattern frequently connected to events like DSGSDs. The understanding of such movement is especially crucial for geohazard monitoring and geomorphological characterization, since it can occur over extended periods and provide serious threats to land stability. This deformation pattern has been confirmed through the PCA analysis carried out on InSAR data. Because of this, it was possible to describe the kinematics of the deformation phenomena and show the roto-translation patterns of the surface processes of the DsGSD. The upper sectors of the slope are characterized by a nearly complete vertical displacement in the descending direction (cluster UP-1). In this instance, horizontal shifts in the central sectors, clusters EW-1 and EW-2, become significant when moving westward. Lastly, the vertical displacement exhibits an upward orientation in the bottom sectors (clusters UP-3 and UP-4) (Figure 4).

Concerning the surficial evidence of the Becca d'Aver, optical multispectral data played an important role. The accumulation of fine-grained soil material near the base of the slope in the Becca d'Aver study area suggests the development of soil horizons in the lower portions, while the upper sectors remain dominated by exposed rock outcrops. The Champagne mixed fan, in the middle of the slope, is a depositional landform where debris from the upper regions has accumulated, increasing the content of clay and organic carbon in the area. Conversely, the very high carbonate content demonstrated the influence of the original material on land degradation, particularly at the slope's peak, where rock outcrops serve as a representation of the primary bare soil areas because of the steep slopes. In this sense, the BSI results, carried out exploiting open-source Sentinel-2 data, reveal high values in the lower parts of the slope. While bare soil is typically linked to rocky outcrops at high elevations, in this case, the spectral signature may result from recently deposited, unconsolidated sediments with poor vegetation cover. On the other hand, the upper slope sectors exhibit lower BSI values due to the combination of the exposed bedrocks and sparse vegetation or the presence of weathered carbonate crusts. This interpretation of soil properties—such as spatial variability in carbonate, clay and iron oxide content—is influenced by the complex lithological setting of the area, characterized by chaotic metamorphic formations. The heterogeneity of these formations plays a key role in shaping both the distribution of bare soil signatures captured by BSI and the varied pedogenic development along the slope. Radar and optical data are important sources of information, especially for non-detailed analysis, the resolution of both sensors being well-suited to large areas. However, for local information, terrain and extremely sensitive instruments are still more powerful in capturing very small features and landforms.

TA allowed us to capture the main common landforms in the area of interest at an appropriate slope-scale resolution and to establish the space and time relations of the processes in the slope morphology. In recent years, the wide availability of DTMs mainly derived from LiDAR acquisitions at regional or national scale allowed a detailed TA. 3D LiDAR-derived products are commonly used for recognition, characterization and extraction (e.g., Glenn et al., 2006; Jaboyedoff et al., 2012; Tarolli, 2014), allowing the representation of the

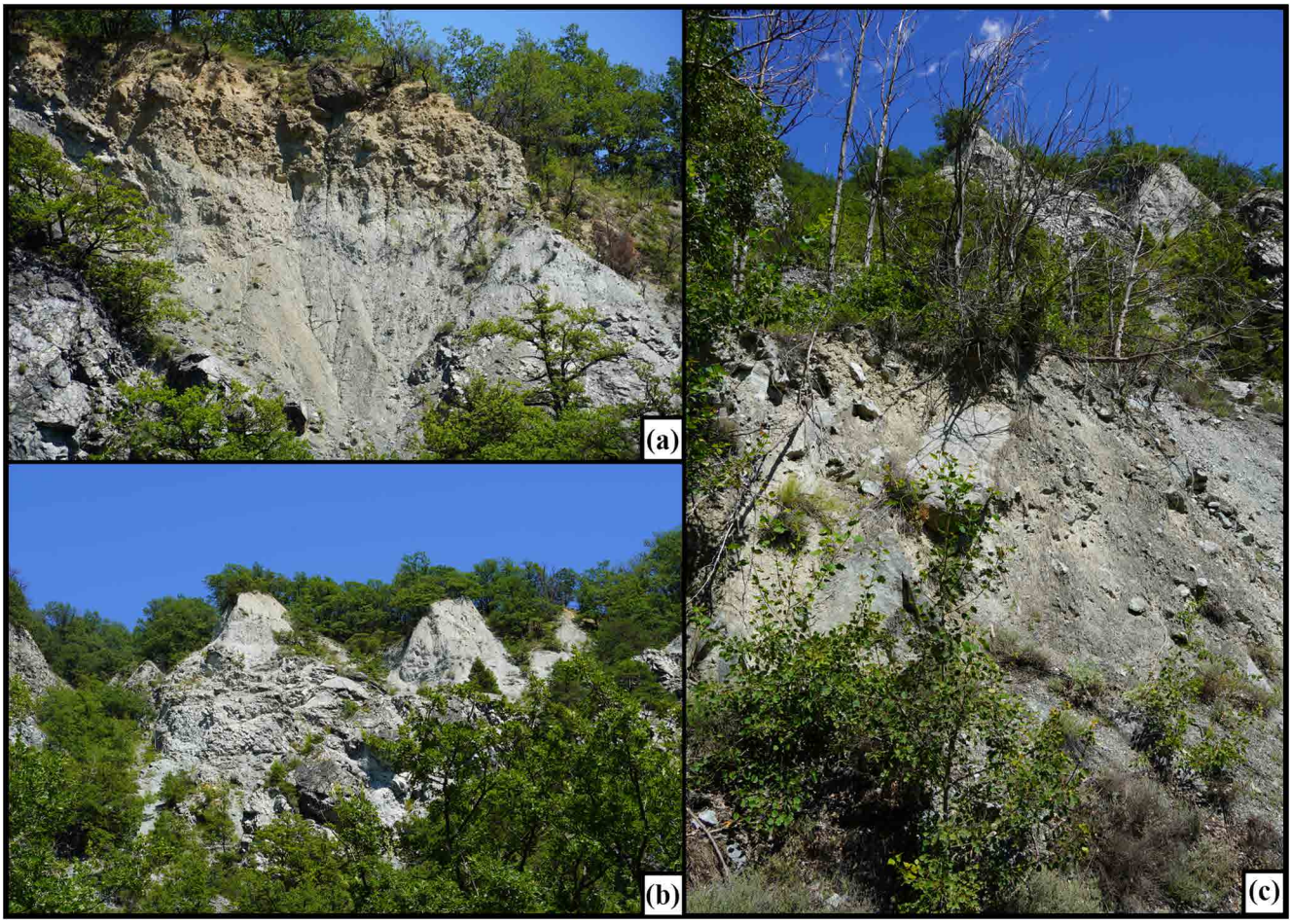

FIGURE 9 Deposits in the pseudo-badlands are highly connected with the drainage. Glacial deposits on top of serpentinites are eroded by rockfalls and rill erosion (a) and assume the typical biancane like shape (b). (c) Waste deposits near an inactive quarry at the toe of pseudo-badlands.

topographical surface through the detection of the geometrically identifiable entities and their relationship.

The combined use of InSAR, BSI and TA guarantees the proper slope-scale survey and definition of the evolution and interrelation of landscape features, allowing the comprehensive knowledge of sediment dynamics and related landforms at Cretaz–Comba Basset Basin scale.

In addition, the 1:10000 scale geomorphological data were stored in the MorphDB directly in the field and represent a usable database for an area characterized by high geomorphological risk. The geomorphological database allows us to represent all the geomorphological processes affecting a portion of slope. Usually, within a traditional geomorphological map only the last or the main morphogenetic process is reported on the map (Castiglioni, 1982). In complex areas affected by DsGSD, geomorphological information is too dense to be simply represented on a map. The problem was initially highlighted by Forno et al. (2022), who support a full coverage cartographic approach with an object-based method.

Within the main map pseudo-badlands were also mapped, with a dedicated symbol, representing the most complex and polygenic landforms in the area. Different authors have already described pseudo-badlands landforms in the Apennine context (Ferrando, Faccini, & Coratza, 2024; Rizzo et al., 2023). The landforms reported in our study crop out in highly fractured metamorphic rocks in an alpine environment. Bollati et al. (2017, 2019) correlates the pseudo-badlands with glacial deposits. We note that the pseudo-badlands are formed in metamorphic rock, even though glacial deposits are in contact with these bedrock formations at the top. Glacial deposits had initially favoured runoff processes and gully formation, which initiated the drainage of the Cretaz–Comba Basset stream. This process has continued to deepen, channels to fractured metamorphic bedrock and accelerating erosive processes, with substantial contributions from slope-associated processes (Figure 9a,b). However, the role of bedrock lithostructure in favouring the occurrence of vertical weakness zones, on which erosion phenomena can more easily occur, should also be considered (e.g., Mariani & Zerboni, 2020).

The GSI analysis revealed that the pseudo-badlands landforms significantly contribute to sediments (blocks) that are available to be transported away by debris flows. The very blocky structure of the bedrock highlighted by the GSI analysis and detected during field surveys is a predisposing factor favouring erosion and rockfalls. In addition, the topographic position of the pseudo-badland's landforms (i.e., crossed by the main drainage) ensures high connectivity with the drainage as shown by the IC model. Finally, waste serpentinite deposits associated with abandoned quarries (Figure 8c) are directly connected to the Cretaz–-Comba Basset stream. Even if along the drainage several check dams are present to limit the effect of debris flow, the geomorphological evidence of the area (i.e., the Champagne Village rises directly on a giant mixed fan) suggests that debris flows

are the main morphogenetic factor and particular attention should be paid to the potential effect of the debris in the village.

In conclusion, this work presents a multi-scale, multi-sensor geomorphological assessment of the Becca d'Aver DsGSD in the Aosta Valley (Italy). The multidisciplinary approach for the morphological and structural characterization of DSGSDs was successfully recently applied in the past in these contexts (Agliardi & Crippa, 2022; Chalupa et al., 2025). The study area here presented is ideal for a multi-scale approach because it is fully characterized by geomorphological processes acting at different spatial and temporal scales. However, a multi-temporal evaluation of the Cretaz–Comba debris flow system in the basin could be conducted in the future using a dedicated multi-temporal analysis approach (e.g., Voglino et al., 2025). The DsGSD affects the entire slope and superimposed on the area is a wide set of other slopes with fluvial and runoff as well as glacial and anthropogenic processes shaping the relief. The geomorphological data were collected in the field and entered into a geomorphological database able to highlight the complex overlap of these geomorphic processes. The area was initially characterized at slope scale with remotely sensed data deriving from different satellite platforms as well as TA. In addition, detailed field surveys were conducted in the Cretaz–Comba Basset basin to fully evaluate the relationship between the landforms and deposits that can produce sediments available to be activated as debris flow. In addition, the IC highlights the importance of pseudo-badlands and waste quarried deposits as sources of sediment, given the high connectivity within the drainage system. The study reveals that a comprehensive geomorphological approach is fundamental in geologically complex areas to accurately evaluate geomorphological processes in time and space in a perspective of applied studies.

AUTHOR CONTRIBUTIONS

Alberto Bosino and Martina Cignetti: writing – original draft, methodology, investigation, data curation and analysis and review and editing. **Danilo Godone, Mattia De Amicis, Federico Raspini and Michael Maerker:** supervision, funding acquisition, formal analysis and conceptualisation. **Francesco Barbadori, Pierluigi Confuorto, Sarah Aliu, Olga Nardini, Ahmed Hafiz, Samuel Pelacani and Daniele Ferrari Trecate:** processing and validation of acquired data and software and formal analysis.

ACKNOWLEDGEMENTS

The authors thank the editor and the reviewers for their useful comments and suggestions that helped to improve the manuscript. This work was supported by: PRIN project 2022C2XPK7 funded by the Italian Ministry of University and Research, entitled 'Full cOveRage, Multi-scAle and multi-sensor geomorphological map: a practical tool for TerrItOrial plaNning - FORMATION'. We thank Laura Ferigato for her help in English language final editing. Open access publishing facilitated by Universita degli Studi di Milano-Bicocca, as part of the Wiley - CRUI-CARE agreement.

CONFLICT OF INTEREST STATEMENT

The authors declare no conflicts of interest.

DATA AVAILABILITY STATEMENT

The data that support the findings of this study are available from the corresponding author upon reasonable request.

REFERENCES

Agliardi, F. & Crippa, C. (2022) Deep-Seated Gravitational Slope Deformations. In: Shroder, J. (Ed.) *Treatise on geomorphology, second edition, eleven volume set*. Oxford: Elsevier, Academic Press, pp. 183–199. Available from: https://doi.org/10.1016/B978-0-12-818234-5.00182-6

Agliardi, F., Crosta, G.B., Zanchi, A. & Ravazzi, C. (2009) Onset and timing of deep-seated gravitational slope deformations in the eastern Alps, Italy. *Geomorphology*, 103(1), 113–129. Available from: https://doi.org/10.1016/j.geomorph.2007.09.015

Aljinović, D., Jurak, V., Mileusnić, M., Slovenec, D. & Presečki, F. (2010) The origin and composition of flysch deposits as an attribute to the excessive erosion of the Slani Potok valley (Salty Creek), Croatia. *Geologia Croatica*, 63(3), 313–322. Available from: https://doi.org/10.4154/gc.2010.25

Battaglia, S., Leoni, L. & Sartori, F. (2002) Mineralogical and grain size composition of clays developing calanchi and biancane erosional landforms. *Geomorphology*, 49(1–2), 153–170. Available from: https://doi.org/10.1016/S0169-555X(02)00171-X

Bell, R.E., Studinger, M., Shuman, C.A., Fahnestock, M.A. & Joughin, I. (2007) Large Subglacial Lakes in East Antarctica at the onset of fast-flowing ice streams. *Nature*, 445(7130), 904–907. Available from: https://doi.org/10.1038/nature05554

Bianchini, M., Morelli, S., Francioni, M. & Bonì, R. (2025) Prediction capability of analytical hierarchy process (AHP) in badland susceptibility mapping: the Foglia River basin (Italy) case of study. *Land*, 14(3), 651. Available from: https://doi.org/10.3390/land14030651

Bishop, M.P., James, L.A., Shroder, J.F., Jr. & Walsh, S.J. (2012) Geospatial technologies and digital geomorphological mapping: concepts, issues and research. *Geomorphology*, 137(1), 5–26. Available from: https://doi.org/10.1016/j.geomorph.2011.06.027

Bistacchi, A., Dal Piaz, G., Massironi, M., Zattin, M. & Balestrieri, M. (2001) The Aosta–Ranzola extensional fault system and Oligocene–present evolution of the Austroalpine–Penninic wedge in the northwestern Alps. *International Journal of Earth Sciences*, 90(3), 654–667. Available from: https://doi.org/10.1007/s005310000178

Bistacchi, A. & Massironi, M. (2001) Introduzione alla tettonica fragile neoalpina e sua influenza sull'instabilità dei versanti. In: Pasquarè, G. (Ed.) *Tettonica recente e instabilità di versante nelle Alpi Centrali*, Italy: GNDT-CNR, Milano, pp. 9–33.

Boehner, J. & Selige, T. (2006) Spatial prediction of soil attributes using terrain analysis and climate regionalisation. In: Boehner, J., McCloy, K.R. & Strobl, J. (Eds.) *SAGA - analysis and modelling applications*, Goettinger Geographische Abhandlungen. Goettingen: Goltze, pp. 13–28.

Bollati, I., Pellegrini, M., Reynard, E. & Pelfini, M. (2017) Water driven processes and landforms evolution rates in mountain geomorphosites: examples from Swiss Alps. *Catena*, 158, 321–339. Available from: https://doi.org/10.1016/j.catena.2017.07.013

Bollati, I.M., Azzoni, R.S., Tagliaferri, A., Tronti, G., Pelfini, M., Vilímek, V., et al. (2024) What do trees reveal about the sliding of the lateral moraine of the belvedere glacier (western Italian Alps)? *AUC Geographica*, 59(1), 1–17. Available from: https://doi.org/10.14712/23361980.2024.14

Bollati, I.M., Masseroli, A., Mortara, G., Pelfini, M. & Trombino, L. (2019) Alpine gullies system evolution: erosion drivers and control factors. Two examples from the western Italian Alps. *Geomorphology*, 327, 248–263. Available from: https://doi.org/10.1016/j.geomorph.2018.10.025

Bosino, A., La Licata, M., Franceschi, L., Hafiz, A., Maggi, V., Maerker, M., et al. (2024) Multi-strata geomorphological database (MorphDB): a methodological breakthrough in geomorphological mapping. *Geografia Fisica e Dinamica Quaternaria*, 47(1), 147–160.

Bryan, R. & Yair, A. (1982) Perspectives on studies of badland geomorphology. In: *BADLAND Geomorhology and piping, edited by Rorke Bryan and Aaron Yair 1982*. Cambridge: University Press.

Bufalini, M., Materazzi, M., De Amicis, M. & Pambianchi, G. (2021) From traditional to modern 'full coverage' geomorphological mapping: a study case in the Chienti river basin (Marche region, Central Italy). *Journal of Maps*, 17(3), 17–28. Available from: https://doi.org/10.1080/17445647.2021.1904020

Bufalini, M., Omran, A. & Bosino, A. (2022) Assessment of Badlands erosion dynamics in the Adriatic side of Central Italy. *Geosciences*, 12(5), 208. Available from: https://doi.org/10.3390/geosciences12050208

Campobasso, C., Carton, A., Chelli, A., D'Orefice, M., Dramis, F., Graciotti, R., et al. (2021) Aggiornamento ed integrazioni delle linee guida della Carta Geomorfologica D'Italia alla scala 1:50000 e banca dati geomorfologica. Quaderni del Servizio Geologico Nazionale, III, 13 (1), Versione 2.0, 153.

Carraro, F. & Perotto, A. (1991) Integrazione del rilevamento geologico-strutturale in scala 1:100.000 relativo ad alcune aree di preminente importanza nella Regione Valle d'Aosta: depositi quaternari. Rapporto inedito, GEODE s.r.l., Milano, 93.

Casagli, N., Frodella, W., Morelli, S., Tofani, V., Ciampalini, A., Intrieri, E., et al. (2017) Spaceborne, UAV and ground-based remote sensing techniques for landslide mapping, monitoring and early warning. *Geoenvironmental Disasters*, 4(1), 9. Available from: https://doi.org/10.1186/s40677-017-0073-1

Castiglioni, G.B. (1982) La cartografia geomorfologica tra ricerca di base e ricerca applicata. *Bollettino. Societa Geologica Italiana*, XI, 609–632.

Cavalli, M., Trevisani, S., Comiti, F. & Marchi, L. (2013) Geomorphometric assessment of spatial sediment connectivity in small Alpine catchments. *Geomorphology*, 188, 31–41. Available from: https://doi.org/10.1016/j.geomorph.2012.05.007

Chalupa, V., Pánek, T., Březný, M., Gutiérrez, F. & Medialdea, A. (2025) Evolution of deep-seated gravitational slope deformation in a deep valley of the Czech flysch Carpathians. *Geomorphology*, 470, 109545. Available from: https://doi.org/10.1016/j.geomorph.2024.109545

Chaussard, E. & Farr, T.G. (2019) A new method for isolating elastic from inelastic deformation in aquifer systems: application to the San Joaquin Valley, CA. *Geophysical Research Letters*, 46(19), 10800–10809. Available from: https://doi.org/10.1029/2019GL084418

Chaussard, E., Wdowinski, S., Cabral-Cano, E. & Amelung, F. (2014) Land subsidence in Central Mexico detected by ALOS InSAR time-series. *Remote Sensing of Environment*, 140, 94–106. Available from: https://doi.org/10.1016/j.rse.2013.08.038

Cignetti, M., Godone, D., Ferrari Trecate, D. & Baldo, M. (2025) New paradigms for geomorphological mapping: a multi-source approach for landscape characterization. *Remote Sensing*, 17(4), 581. Available from: https://doi.org/10.3390/rs17040581

Cignetti, M., Godone, D., Notti, D., Giordan, D., Bertolo, D., Calò, F., et al. (2023a) State of activity classification of deep-seated gravitational slope deformation at regional scale based on Sentinel-1 data. *Landslides*, 20(12), 2529–2544. Available from: https://doi.org/10.1007/s10346-023-02114-7

Cignetti, M., Godone, D., Notti, D., Zucca, F., Meisina, C., Bordoni, M., et al. (2023b) Damage to anthropic elements estimation due to large slope instabilities through multi-temporal A-DInSAR analysis. *Natural Hazards*, 115(3), 2603–2632. Available from: https://doi.org/10.1007/s11069-022-05655-7

Cignetti, M., Godone, D., Zucca, F., Bertolo, D. & Giordan, D. (2020) Impact of deep-seated gravitational slope deformation on urban areas and large infrastructures in the Italian Western Alps. *Science of the Total Environment*, 740, 140360. Available from: https://doi.org/10.1016/j.scitotenv.2020.140360

Coratza, P., Bollati, I.M., Panizza, V., Brandolini, P., Castaldini, D., Cucchi, F., et al. (2021) Advances in geoheritage mapping: application to iconic geomorphological examples from the Italian landscape. *Sustainability*, 13(20), 11538. Available from: https://doi.org/10.3390/su132011538

Coratza, P. & Parenti, C. (2021) Controlling factors of badland morphological changes in the Emilia Apennines (northern Italy). *Water*, 13(4), 539. Available from: https://doi.org/10.3390/w13040539

Cornamusini, G., Conti, P., Bonciani, F., Callegari, I., Carmignani, L., Martelli, L., et al. (2009) Note Illustrative Della Carta Geologica d'Italia Alla Scala 1: 50.000 "Foglio 267-San Marino". Servizio Geologico d'Italia: Rome, Italy, 2009.

Crema, S. & Cavalli, M. (2018) SedInConnect: a stand-alone, free and open source tool for the assessment of sediment connectivity. *Computers & Geosciences*, 111, 39–45. Available from: https://doi.org/10.1016/j.cageo.2017.10.009

Crosetto, M., Solari, L., Mróz, M., Balasis-Levinsen, J., Casagli, N., Frei, M., et al. (2020) The evolution of wide-area DInSAR: From regional and national services to the European Ground Motion Service. *Remote Sensing*, 12(12), 2043.

Crosta, G.B., Frattini, P. & Agliardi, F. (2013) Deep seated gravitational slope deformations in the European Alps. *Tectonophysics*, 605, 13–33. Available from: https://doi.org/10.1016/j.tecto.2013.04.028

Dal Piaz, G., Gianotti, F., Monopoli, B., Pennacchioni, G., Tartarotti, P., Schiavo, A., et al. (2010) Note Illustrative della CARTA GEOLOGICA D'ITALIA alla scala 1: 50.000: foglio 091 CHATILLON. ISPRA - Serv. Geol. D'It., Roma.

Diek, S., Fornallaz, F., Schaepman, M.E. & De Jong, R. (2017) Barest pixel composite for agricultural areas using Landsat time series. *Remote Sensing*, 9(12), 1245. Available from: https://doi.org/10.3390/rs9121245

Dill, H.G., Andrei, B., Sorin-Ionut, B., Kristian, U., Jorge, G.T., Daniel, B. & Thomas, C. (2020) The "badland trilogy" of the Desierto de la Tatacoa, upper Magdalena Valley, Colombia, a result of geodynamics and climate: With a review of badland landscapes. *Catena*, 194, 104696.

Discenza, M.E., Esposito, C., Di Luzio, E., Delchiaro, M., Di Martire, D., Minnillo, M., et al. (2023) Deep-seated gravitational slope deformations in Molise region (Italy): novel inventory and main geomorphological features. *Journal of Maps*, 19(1), 2163198. Available from: https://doi.org/10.1080/17445647.2022.2163198

ESRI. (2011) ArcGIS Desktop: Release 10. Redlands, CA: Environmental Systems Research Institute.

Ferrando, A., Faccini, F. & Coratza, P. (2024) Ophiolites: geological heritage with multifaceted cultural values. *Geoheritage*, 16(4), 108. Available from: https://doi.org/10.1007/s12371-024-01009-w

Festa, D. & Del Soldato, M. (2023) EGMStream, a desktop app for EGMS data downstream. *Remote Sensing*, 15(10), 2581. Available from: https://doi.org/10.3390/rs15102581

Fialko, Y., Sandwell, D., Simons, M. & Rosen, P. (2005) Three-dimensional deformation caused by the bam, Iran, earthquake and the origin of shallow slip deficit. *Nature*, 435(7040), 295–299. Available from: https://doi.org/10.1038/nature03425

Fiaschi, S. & Wdowinski, S. (2020) Local land subsidence in Miami Beach (FL) and Norfolk (VA) and its contribution to flooding Hazard in coastal communities along the U.S. Atlantic Coast. *Ocean and Coastal Management*, 187, 105078. Available from: https://doi.org/10.1016/j.ocecoaman.2019.105078

Forno, M.G., Fubelli, G., Gattiglio, M., Taddia, G. & Ghignone, S. (2022) Object-based geomorphological mapping: application on an Alpine deep-seated gravitational slope deformation contest (Germanasca Valley, Western Alps, Italy). *Applied Sciences*, 12(2), 778. Available from: https://doi.org/10.3390/app12020778

Gianotti, F., Forno, M.G., Ivy-Ochs, S. & Kubik, P.W. (2008) New chronological and stratigraphical data on the Ivrea amphitheatre (Piedmont, NW Italy). *Quaternary International*, 190(1), 123–135. Available from: https://doi.org/10.1016/j.quaint.2008.03.001

Giardino, M., Ratto, S., Palomba, M., Alberto, W., Armand, M. & Cignetti, M. (2013) The debris flows inventory of the aosta valley region: An integrated natural hazards assessment. In: *Landslide science and practice: volume 1: landslide inventory and susceptibility and Hazard zoning*. Berlin, Heidelberg: Springer Berlin Heidelberg, pp. 127–134.

Glenn, N.F., Streutker, D.R., Chadwick, D.J., Thackray, G.D. & Dorsch, S.J. (2006) Analysis of LiDAR-derived topographic information for characterizing and differentiating landslide morphology and activity. *Geomorphology*, 73(1-2), 131–148.

Guth, P.L., Van Niekerk, A., Grohmann, C.H., Muller, J.P., Hawker, L., Florinsky, I.V., et al. (2021) Digital elevation models: terminology and definitions. *Remote Sensing*, 13(18), 3581.

Guzzetti, F., Mondini, A.C., Cardinali, M., Fiorucci, F., Santangelo, M. & Chang, K.T. (2012) Landslide inventory maps: new tools for an old problem. *Earth-Science Reviews*, 112(1–2), 42–66. Available from: https://doi.org/10.1016/j.earscirev.2012.02.001

Hilley, G.E., Bürgmann, R., Ferretti, A., Novali, F. & Rocca, F. (2004) Dynamics of slow-moving landslides from permanent Scatterer

analysis. *Science*, 304(5679), 1952–1955. Available from: https://doi.org/10.1126/science.1098821

CARG GATE. https://progetto-carg.isprambiente.it/cartografiaCARG/cartageologica.php?regione=Valle+d%27Aosta&foglio=091

Jaboyedoff, M., Oppikofer, T., Abellán, A., Derron, M.H., Loye, A., Metzger, R., et al. (2012) Use of LIDAR in landslide investigations: a review. *Natural Hazards*, 61(1), 5–28. Available from: https://doi.org/10.1007/s11069-010-9634-2

La Licata, M., Bosino, A., Bettoni, M. & Maerker, M. (2023) Assessing landscape features and geomorphic processes influencing sediment dynamics in a geomorphologically highly active Mediterranean agroecosystem: the upper Val d'Arda case study (northern Apennines, Italy). *Geomorphology*, 433, 108724. Available from: https://doi.org/10.1016/j.geomorph.2023.108724

La Licata, M., Bosino, A., De Amicis, M., Terret, A. & Maerker, M. (2025) A GIS-based multiscale mapping framework to assess and visualize complex and polygenetic geomorphic systems–a novel 'geomorphic entities' approach. *Journal of Maps*, 21(1), 2437256. Available from: https://doi.org/10.1080/17445647.2024.2437256

Maerker, M., Schillaci, C., Melis, R.T., Kropáček, J., Bosino, A., Vilímek, V., et al. (2019) Geomorphological processes, forms and features in the surroundings of the Melka Kunture Palaeolithic site, Ethiopia. *Journal of Maps*, 15(2), 797–806. Available from: https://doi.org/10.1080/17445647.2019.1669497

Mariani, G.S. & Zerboni, A. (2020) Surface geomorphological features of deep-seated gravitational slope deformations: a look to the role of lithostructure (N Apennines, Italy). *Geosciences*, 10(9), 334. Available from: https://doi.org/10.3390/geosciences10090334

Marinos, P., Marinos, V. & Hoek, E. (2007) The Geological Strength Index (GSI): a characterization tool for assessing engineering properties for rock masses. In Proceedings International Workshop on Rock Mass Classification for Underground Mining, Mark, Pakalnis and Tuchman (editors), Information Circular (Vol. 9498, pp. 87–94).

McCerery, R., Davies, B.J., Lovell, H., Calvo-Ryan, R., Pearce, D.A., Małecki, J., et al. (2025) Landsystem models from remote and field based geomorphological mapping reveal diverse glacier dynamics on Svalbard. *Geomorphology*, 484, 109854.

Moore, I.D., Grayson, R.B. & Ladson, A.R. (1991) Digital terrain modelling: a review of hydrogical, geomorphological, and biological applications. *Hydrological Processes*, 5(1), 3–30.

Moreno-de las Heras, M. & Gallart, F. (2018) The origin of badlands. In: *Badlands dynamics in a context of global change*. Netherland: Elsevier, pp. 27–59.

Moretti, S. & Rodolfi, G. (2000) A typical "calanchi" landscape on the eastern Apennine margin (Atri, Central Italy): geomorphological features and evolution. *Catena*, 40(2), 217–228. Available from: https://doi.org/10.1016/S0341-8162(99)00086-7

Mortara, G. & Sorzana, P.F. (1987) Fenomeni di deformazione gravitativa profonda nell'arco alpino occidentale italiano. Considerazioni litostrutturali e morfologiche. *Bollettino Della Societa Geologica Italiana*, 106(1987), 303–314.

Pells, S.E., Douglas, K., Pells, P.J., Fell, R. & Peirson, W.L. (2017) Rock mass erodibility. *Journal of Hydraulic Engineering*, 143(5), 06016031. Available from: https://doi.org/10.1061/(asce)hy.1943-7900.0001243

Quesada-Román, A. & Peralta-Reyes, M. (2023) Geomorphological mapping global trends and applications. *Geographies*, 3(3), 610–621. Available from: https://doi.org/10.3390/geographies3030032

Rączkowska, Z. & Zwoliński, Z. (2015) Digital geomorphological map of Poland. *Geographia Polonica*, 88(2), 205–210. Available from: https://doi.org/10.7163/GPol.0025

Rafiei Renani, H. & Cai, M. (2022) Forty-year review of the Hoek–Brown failure criterion for jointed rock masses. *Rock Mechanics and Rock Engineering*, 55(1), 439–461.

Ratto, S., Bonetto, F. & Comoglio, C. (2003) The october 2000 flooding in Aosta Valley (Italy): event description and land planning measures for the risk mitigation. *International Journal of River Basin Management*, 1(2), 105–116.

Reddy, G.O. (2018) *Geospatial technologies in land resources mapping, monitoring, and management: an overview*. Switzerland: Springer International Publishing, pp. 1–18.

Rizzo, G., Buccione, R., Dichicco, M., Punturo, R. & Mongelli, G. (2023) Petrography, geochemistry and mineralogy of serpentinite rocks exploited in the ophiolite units at the Calabria-Basilicata boundary, southern Apennine (Italy). *Fibers*, 11(10), 81. Available from: https://doi.org/10.3390/fib11100081

Servizio Geologico d'Italia. (2010) Carta Geologica d'Italia alla scala 1: 50.000 - Foglio 91 "Châtillon". ISPRA- Servizio Geologico d'Italia. Regione Autonoma Aosta Valley. LTS - Land Technology & Services Srl.

Siart, C., Bubenzer, O. & Eitel, B. (2009) Combining digital elevation data (SRTM/ASTER), high resolution satellite imagery (Quickbird) and GIS for geomorphological mapping: a multi-component case study on Mediterranean karst in Central Crete. *Geomorphology*, 112(1–2), 106–121. Available from: https://doi.org/10.1016/j.geomorph.2009.05.010

Tarolli, P. (2014) High-resolution topography for understanding earth surface processes: opportunities and challenges. *Geomorphology*, 216, 295–312.

Voglino, B., Godone, D., Baldo, M., Bono, B., Luino, F., Bonomelli, R., et al. (2025) Application of structure from motion techniques using historical aerial images, orthomosaics, and aerial LiDAR point cloud datasets for the investigation of debris flow source areas. *Remote Sensing*, 17(22), 3658. Available from: https://doi.org/10.3390/rs17223658

Wang, L. & Liu, H. (2006) An efficient method for identifying and filling surface depressions in digital elevation models for hydrologicanalysis and modelling. *International Journal of Geographical Information Science*, 20(2), 193–213. Available from: https://doi.org/10.1080/13658810500433453

Zevenbergen, L.W. & Thorne, C.R. (1987) Quantitative analysis of land surface topography. *Earth Surface Processes and Landforms*, 12(1), 47–56. Available from: https://doi.org/10.1002/esp.3290120107

SUPPORTING INFORMATION

Additional supporting information can be found online in the Supporting Information section at the end of this article.

How to cite this article: Bosino, A., Barbadori, F., Confuorto, P., Godone, D., De Amicis, M., Raspini, F. et al. (2026) Geomorphological mapping of the Becca d'Aver deep-seated gravitational slope deformation (Aosta Valley, Italy) based on multi-scale and multi-sensor analysis. *Earth Surface Processes and Landforms*, 51(5), e70298. Available from: https://doi.org/10.1002/esp.70298